Journal of Thermal Analysis and Calorimetry (2018) 133:813–821
https://doi.org/10.1007/s10973-018-7229-4

Synthesis and characterization of copper, nickel, cobalt, zinc complexes with 4-nitro-3-pyrazolecarboxylic acid ligand

Željko Jaćimović[1] · Milica Kosović[1] · Vlatko Kastratović[2] · Berta Barta Holló[3] · Katalin Mészáros Szécsényi[3] · Imre Miklós Szilágyi[4,5] · Nedeljko Latinović[6] · Ljiljana Vojinović-Ješić[3] · Marko Rodić[3]

Received: 15 August 2017 / Accepted: 30 March 2018 / Published online: 11 April 2018

Abstract

In the continuation of our systematic research of pyrazole coordination compounds, complexes of Cu(II), Ni(II), Co(II) and Zn(II) with 4-nitro-3-pyrazolecarboxylic acid ligand (L) were synthesized in the reaction of warm ethanolic solutions of the ligand and $CuCl_2{\cdot}2H_2O$, $Ni(CH_3COO)_2$, $CoCl_2{\cdot}6H_2O$ and $Zn(CH_3COO)_2$, mixed in the metal-to-ligand ratio of 1:2. As the compounds could not be obtained in the form suitable for single-crystal structure analysis, their bis(ligand) structures, ML_2 ($M = Cu^{II}$, Ni^{II}, Co^{II} and Zn^{II}) were proposed on the basis of elemental analysis, IR spectrometry, conductometric and TG–MS measurements. The low conductivity of the compounds additionally supports the deprotonation of the ligand and the formation of neutral complexes. The solvent content was calculated using the thermogravimetric (TG) data. According to TG data, the copper(II) compound crystallizes with 8 while nickel(II) complex with 4 water molecules, $CuL_2{\cdot}8H_2O$, $NiL_2{\cdot}4H_2O$. Complexes of Co(II) and Zn(II) contain 1 and 1.5 water molecules. Despite the differences in solvation properties, the high similarity in the course of the decomposition refers to the similar coordination mode of the organic ligand. The crystal and molecular structures of $HL{\cdot}H_2O$ and $NH_4[LHL]$ were determined by single-crystal X-ray structure analysis. Biological research based on determining the inhibition effect of commercial fungicide Cabrio top, ligand, and all newly synthesized complexes on *Ph. viticola* has been carried out using the phytosanitary method.

Keywords Coordination complexes · Pyrazole-type ligand · Thermal properties · TG–MS

Introduction

The reason why we focus our research on the transition metal complexes with pyrazole derivatives is the theoretical and practical significance of these compounds. A number of pyrazole derivatives show biological activity and, as a consequence, among them are commercial products or compounds in the phase of the evaluation of their activity. Their representatives show antipyretic [1, 2], antirheumatic [3] and antimicrobial [4] behaviors. Some of them are active ingredients of products with potential antitumor activity [5–7]. In agriculture, they are in the use as pesticides [8–10]. As pyrazoles readily form complexes, they are suitable agents to investigate the active cites of biomolecules [11] and for modeling the biosystems of oxygen transfer [12]. In living organisms, metal ions are usually bonded to the imidazole part of the histidine, which is a part of the proteins. In view of the similarity of pyrazole with imidazole [13], they are suitable to mimic enzymatic reactions. The thermal properties [14–18] of

Electronic supplementary material The online version of this article (https://doi.org/10.1007/s10973-018-7229-4) contains supplementary material, which is available to authorized users.

✉ Željko Jaćimović
zeljkoj@ac.me

[1] Faculty of Metallurgy and Technology, University of Montenegro, Podgorica, Montenegro

[2] Faculty of Natural Sciences, University of Montenegro, Podgorica, Montenegro

[3] Faculty of Sciences, University of Novi Sad, Novi Sad, Serbia

[4] Department of Inorganic and Analytical Chemistry, Budapest University of Technology and Economics, Budapest, Hungary

[5] MTA-BME Research Group of Technical Analytical Chemistry, Budapest, Hungary

[6] Biotechnical Faculty, University of Montenegro, Podgorica, Montenegro

new compounds very often limit their practical applicability as neither physical nor chemical changes can occur in the temperature range of the usage. In our previous study, we described a solvent exchange reaction in some pyrazole complexes with a remarkable antifungal property. In this paper, we describe the syntheses of four new complex compounds of formula $CuL_2{\cdot}8H_2O$, $NiL_2{\cdot}4H_2O$, $CoL_2{\cdot}H_2O$, $ZnL_2{\cdot}1.5H_2O$ with a pyrazole-based **L** = 4-nitro-3-pyrazolecarboxylic acid ligand (L). The compounds were characterized by elemental analysis, IR spectrometry, conductometric and TG–MS measurements coupled to mass spectrometer (TG–MS). The crystal and molecular structures of $HL{\cdot}H_2O$ and NH_4[LHL] were determined by single-crystal X-ray structure analysis. The antifungal activity ligand and of all compounds were tested for fungi *Ph. viticola* using the phytosanitary method.

Experimental

Preparation of complexes

Complex $CuL_2{\cdot}8H_2O$ was synthesized in the reaction on the warm ethanolic solutions of $CuCl_2{\cdot}2H_2O$ and 4-nitro-3-pyrazolecarboxylic acid ligand (L) mixed in molar ratio 1:2. After 2 days, the microcrystalline product was filtered off and washed with ethanol. Complex $NiL_2{\cdot}4H_2O$ was synthesized in the reaction on the warm ethanolic solutions of $Ni(CH_3COO)_2$ and 4-nitro-3-pyrazolecarboxylic acid ligand (L) mixed in molar ratio 1:2. After 6 h, the microcrystalline product was filtered off and washed with ethanol. Complex $CoL_2{\cdot}H_2O$ was synthesized in the reaction on the warm ethanolic solutions of $CoCl_2{\cdot}6H_2O$ and 4-nitro-3-pyrazolecarboxylic acid ligand (L) mixed in molar ratio 1:2. After 8 h, the microcrystal product was filtered off and washed with ethanol. Complex $ZnL_2{\cdot}1.5H_2O$ was synthesized in the reaction on the warm ethanolic solutions of $Zn(CH_3COO)_2$ and 4-nitro-3-pyrazolecarboxylic acid ligand (L) mixed in molar ratio 1:2. After 1 day, the microcrystal product was filtered off and washed with ethanol. Single crystal of the ligand $HL{\cdot}H_2O$ was obtained by recrystallization from ethanol. Single crystal of NH_4[LHL] was obtained in reaction $Zn(NO_3)_2$ with 4-nitro-3-pyrazolecarboxylic acid ligand (L) in the presence of NH_4SCN.

Elemental analysis and molar conductivity data:

$CoL_2{\cdot}H_2O$: found C 24.82%, N 21.72%, H 1.93% calculated for $CoC_8N_6H_4O_8{\cdot}H_2O$ (Mr = 389.10 g mol^{-1}), C 24.69%, N 21.60% and H 1.56%. λ_M (DMF) = 6 Scm^2 mol^{-1} (nonelectrolyte).

$NiL_2{\cdot}4H_2O$: found C 22.32%, N 18.99%, H 3.02%, calculated for $NiC_8N_6H_4O_8{\cdot}4H_2O$ (Mr = 442.91 g mol^{-1}), C 21.69%, N 18.98% and H 2.74%. λ_M (DMF) = 10 Scm^2 mol^{-1} (nonelectrolyte).

$CuL_2{\cdot}8H_2O$: found C 16.69%, N 14.44%, H 3.56%, calculated for $CuC_8N_6H_4O_8{\cdot}8H_2O$ (Mr = 519.82 g mol^{-1}), C 18.48%, N 16.17% and H 3.89%. This compound is not soluble in MeOH, EtOH, H_2O, Me_2CO, MeCN, DMF.

$ZnL_2{\cdot}1.5H_2O$: found C 23.64%, N 20.89%, H 1.98%, calculated for $ZnC_8N_6H_4O_8{\cdot}1.5H_2O$ (Mr = 404.58 g mol^{-1}), C 23.75%, N 20.78% and H 1.75%.

Measurements

Elemental analysis (C, H and N) of air-dried compounds was carried out by standard micromethods.

The molar conductivity of freshly prepared 1×10^{-3} mol dm^{-3} solutions of the complexes in *N*,*N*′-dimethylformamide (DMF) was determined at room temperature using a digital conductivity meter Jenway 4510.

IR data were collected on a Thermo Scientific Nicolet 6700 FTIR spectrometer at room temperature using KBr disks in the range of 4000–400 cm^{-1}. In all the measurements, a resolution of 4 cm^{-1} was applied.

TG–DSC measurements were taken using a TA Instruments SDT Q600 thermal analyzer with a 20 °C min^{-1} heating rate in the range from room temperature to 600 °C, sample mass $\sim$ 1 mg, carrier gas of nitrogen (flow rate: 100 cm^3 min^{-1}), sample holder/reference of alumina crucible/empty alumina crucible. The TG–DSC–MS measurements were taken with the same thermal analyzer coupled online with Hiden Analytical HPR-20/QIC mass spectrometer. The mass spectra were recorded in multiple ion detection (MID) mode by SEM detector. The heating rate was changed to 10 °C min^{-1} and the nitrogen purge gas flow to 50 cm^3 min^{-1}. About 1.5 mg of samples was used.

Biological activity based on determining the inhibition effect of the commercial fungicide Cabrio top and the newly synthesized complexes on *Ph. viticola* has been carried using the phytosanitary method. The diameters of fungal mycelium *Ph. Vitiocola* as parameters of the inhibition effect were processed using the variance analysis, while the testing was performed using the LSD test [19].

Discussion

Crystal structure determination

Diffraction experiments were performed on an Oxford Diffraction Gemini S diffractometer, equipped with sealed-tube X-ray source (Mo$K\alpha$, λ = 0.71073 Å) and a Sapphire3

Table 1 Crystal data and structure refinement details for **HL·H$_2$O** and **NH$_4$[LHL]**

	HL·H$_2$O	**NH$_4$[LHL]**
Chemical formula	$C_4H_5N_3O_5$	$C_8H_9N_7O_8$
M_r	175.11	331.22
Crystal system	Orthorhombic	Monoclinic
Space group	$Pca2_1$	$C2/c$
T/K	295(2)	295(2)
a/Å	12.8499(4)	27.9726(11)
b/Å	3.6213(2)	6.6618(2)
c/Å	29.7140(11)	6.7796(3)
α/°	90	90
β/°	90	90.772(4)
γ/°	90	90
V/Å^3	1382.69(10)	1263.25(8)
Z	8	4
Crystal shape	Trapezoid	Plate
Crystal color	Colorless	Colorless
Crystal size/mm	0.41 × 0.34 × 0.26	0.46 × 0.45 × 0.11
D_c/g cm^{-3}	1.682	1.742
μ/mm^{-1}	0.16	0.16
Absorption correction	Multi-scan	Multi-scan
T_{max}, T_{min}	1.000, 0.932	1.000, 0.934
θ range/°	2.7–28.7	2.9–29.1
Reflections collected	6404	6181
Independent reflections	2751	1518
R_{int}	0.021	0.019
Completeness to θ = 26.3°	99.9	99.6
R_1 [$I > 2\delta(I)$]	0.047	0.068
R_1 [all data]	0.053	0.072
wR_2 [$I > 2\delta(I)$]	0.130	0.175
wR_2 [all data]	0.138	0.177
S	1.035	1.157
Restraints, parameters	9, 223	4, 121
H-atom treatment	Constr.	Mixed
$\Delta\rho_{max}$, $\Delta\rho_{min}$/eÅ^{-3}	0.38, − 0.22	0.38, − 0.35
Flack x	Meaningless	–

area detector, at room temperature. Data collection and reduction were processed with the *CrysAlisPRO* [20]. Structures were solved with the *SHELXT* [21], refined with the *SHELXL*-2017 [22], with the *ShelXle* [23] as the graphical user interface. Structural models were validated by using *PLATON* [24] and *Mercury CSD* [25]. Molecular graphics were produced by *ORTEP* for Windows [26].

A summary of the crystallographic data is given in Table 1. Crystallographic data for **HL·H$_2$O** and **NH$_4$[LHL]** have been deposited with the Cambridge Crystallographic Data Centre as Supplementary Publication Nos. CCDC 1568450 and 1568451, respectively. A copy of these data free of charge can be obtained via https://summary.ccdc.cam.ac.uk/structure-summary form, or by emailing data_request@ccdc.cam.ac.uk.

Molecular structures of **HL·H$_2$O** and **NH$_4$[LHL]** are depicted in Fig. 1, while selected parameters of the molecular geometry are listed in Table 2.

The asymmetric unit of **HL·H$_2$O** consists of two independent 4-nitro-3-pyrazolecarboxylic acids molecules and two water molecules, all of them located in general positions. The two molecules have similar bond lengths and valence angles, which are also in concordance with the structures of 1-methyl-4-nitro-3- and -5-pyrazolecarboxylic acids [27]. The molecules are not planar, as both carboxylic and nitro moieties are twisted along C3–C6 and C4–N3 bonds, with corresponding torsion angles: τ(C3A–C4A–

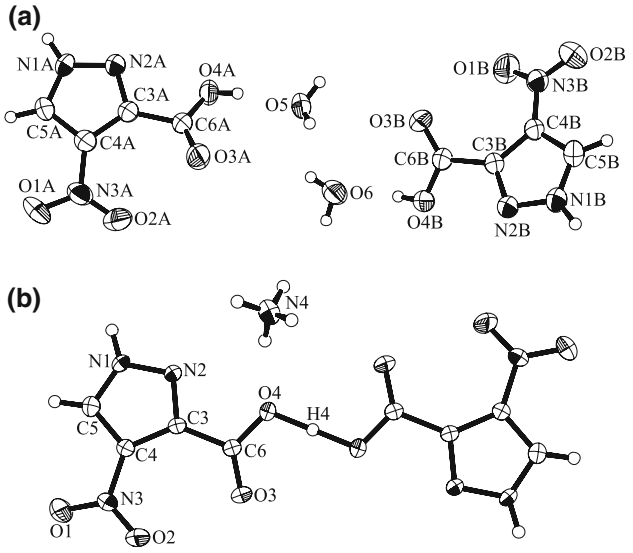

Fig. 1 Molecular structures and the atom numbering scheme of: **a** $HL{\cdot}H_2O$ (all independent molecules of asymmetric unit are shown); **b** NH_4[LHL] (atoms N4 an H4 lie on centers of symmetry). Displacement ellipsoids are shown at the 50% probability level

where all possible hydrogen bond donors and acceptors are involved in interactions (Table S1 in SI).

The asymmetric unit of **NH_4[LHL]** contains half of NH_4^+ cation and half of $[L{\cdots}H{\cdots}L]^-$ anion, as corresponding nitrogen and hydrogen atoms are situated at crystallographic inversion centers. The bond lengths in **NH_4[LHL]** are comparable to those found in **$HL{\cdot}H_2O$**. When compared with the structure of **$HL{\cdot}H_2O$**, it is evident that carboxylate and nitro moieties are less twisted along C3–C6 and C4–N3 bonds, with corresponding torsion angles: τ(C3–C4–N3–O2) = 8.7(6)°, and τ(C4–C3–C6–O3) = 4.9(6)°. In addition to the electrostatic interactions, the crystal structure of **NH_4[LHL]** is further stabilized by numerous hydrogen bonds, where all possible hydrogen bonds such as donors and acceptors are involved in interactions (Table S2 in Supporting Information, SI).

The structure of the coordination compounds with **HL** is presented in Fig. 2. The ligand coordinates in a bidentate fashion through the deprotonated carboxylate group and the N2 atom of the pyrazole moiety. The formation of

Table 2 Selected bond lengths for **$HL{\cdot}H_2O$** and **NH_4[LHL]** (Å)

	$HL{\cdot}H_2O$ (molecule A)	$HL{\cdot}H_2O$ (molecule B)	NH_4[LHL]
N1–N2	1.349(6)	1.341(6)	1.350(3)
N2–C3	1.320(5)	1.333(5)	1.335(3)
C3–C4	1.433(5)	1.405(6)	1.411(4)
C4–C5	1.392(6)	1.366(6)	1.375(4)
C5–N1	1.318(7)	1.328(8)	1.323(4)
C4–N3	1.395(6)	1.424(5)	1.433(4)
N3–O1	1.236(7)	1.215(7)	1.215(4)
N3–O2	1.234(5)	1.211(5)	1.207(4)
C3–C6	1.494(5)	1.487(5)	1.498(4)
C6–O3	1.199(4)	1.204(4)	1.206(3)
C6–O4	1.300(5)	1.300(6)	1.288(3)

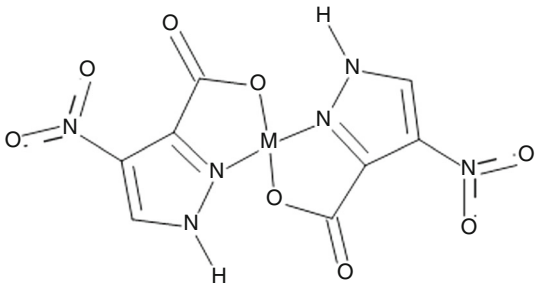

Fig. 2 Coordination of **HL** to metal center (M = Co, Ni, Cu, Zn)

N3A–O2A) = − 12.7(7)°, τ(C3B–C4B–N3B–O2B) = − 12.0(7)°, and τ(C4A–C3A–C6A–O3A) = − 25.6(7)°, τ(C4B–C3B–C6B–O3B) = − 22.3(7)°. Crystal structure of **$HL{\cdot}H_2O$** is stabilized with 3D hydrogen bonding network,

neutral complexes is supported with their very low conductivity values. All compounds contain adsorbed or lattice water.

The FTIR spectra of the complexes are in the accordance with the proposed structure. The characteristic vibrations are listed in Table 3. They show some differences in the region of νOH and νNH bands above 3000 cm^{-1} due to the different numbers and strengths of the hydrogen bonds. Bands appearing in the region below 1700 cm^{-1} are of very similar shape and suggest the same coordination mode of the ligand to the metal ions (Fig. 3).

Thermal data

The thermal properties of the coordination compounds of Co(II), Ni(II), Cu(II) and Zn(II) were measured in dynamic

Table 3 Characteristic vibration bands of the compounds

Band assignments	Wavenumbers/cm^{-1}			
	$CoL_2{\cdot}H_2O$	$NiL_2{\cdot}4H_2O$	$CuL_2{\cdot}8H_2O$	$ZnL_2{\cdot}1.5H_2O$
νOH	3371	3617–3520	3516	3616–3403
νNH	3168–3125	3222–3162	3382–3280	3218–2963
νC=O	1660–1606	1680–1628	1661–1622	1662–1615
νN=O	1537–1353	1543–1351	1543–1296	1538–1357
νN–O	1121	1123–1081	1133	1121

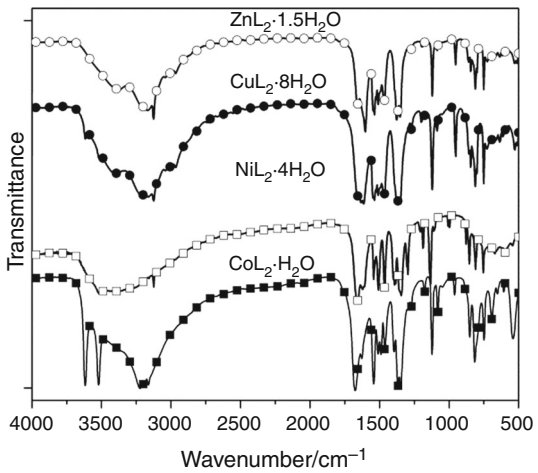

Fig. 3 FTIR spectra of the coordination compounds

loss starting almost at room temperature. The copper(II) compound to ~ 85 °C loses 26.6% in one step, which is in good agreement with the calculated water content (27.70%).

The water evaporation in nickel(II) complex takes place in two well-separated steps releasing 2 water molecules (~ 8%) in each step to 160 °C (calcd. for 4 water molecules: 16.27%). A typical TG–DTG–DSC curve for the decomposition of the nickel(II) compound is presented in Fig. 4. It shows the well-separated peaks for water evaporation with the corresponding mass loss. The anhydrous compound is stable in the temperature range of 160 °C to about 260 °C. At the beginning of the decomposition of NiL_2, the relatively intensive DTG peaks are accompanied with hardly detectable exothermic processes. However,

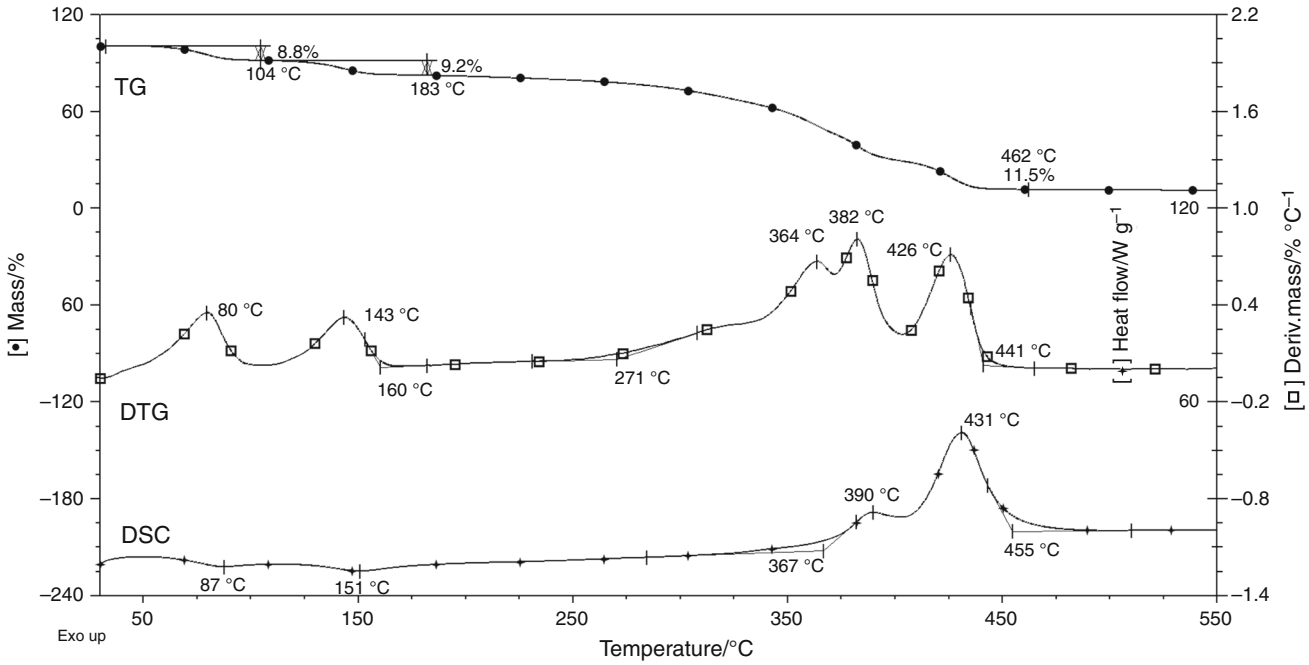

Fig. 4 TG–DTG–DSC curves of $NiL_2{\cdot}4H_2O$ complex

atmosphere of nitrogen. The compounds with Cu(II) and Ni(II) metal centers, $CuL_2{\cdot}8H_2O$ and $NiL_2{\cdot}4H_2O$, in accordance with the proposed composition show a mass almost explosive-like exothermic processes take place above 370 °C, indicating the highly oxidative character of the nitro-substituent of the ligand.

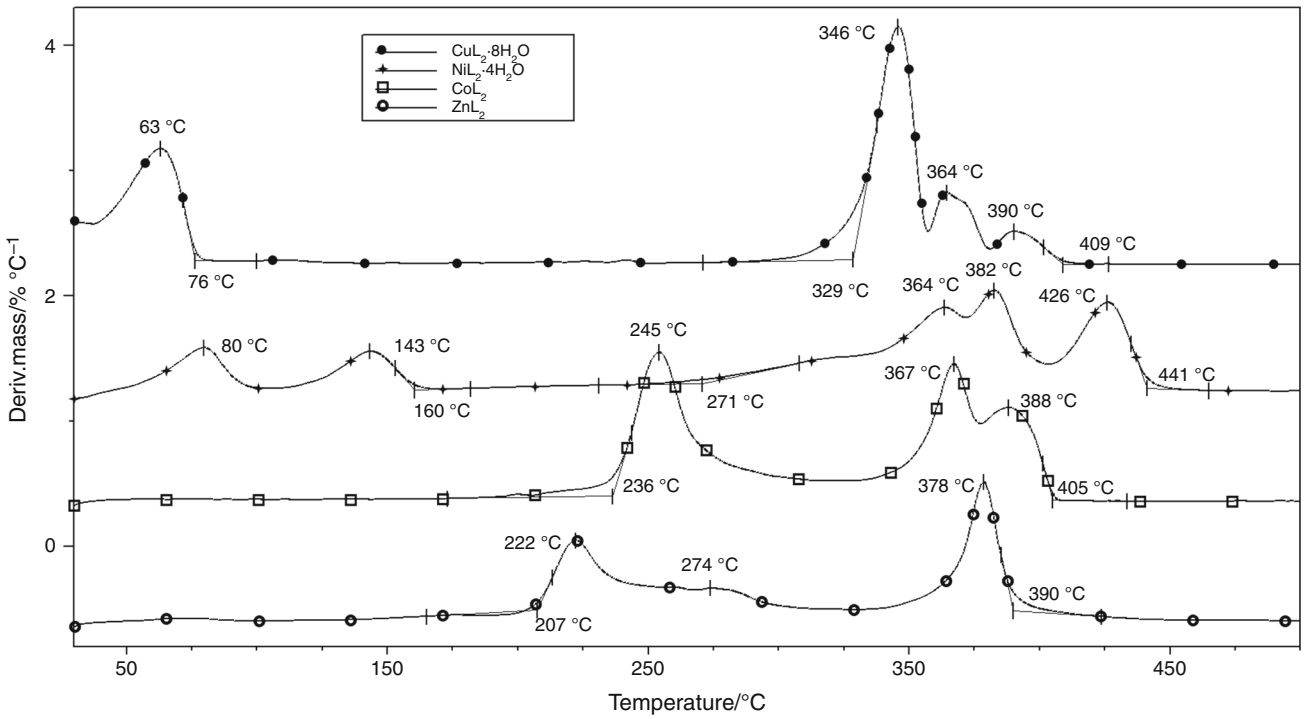

Fig. 5 DTG curves of the compounds in nitrogen atmosphere. For the sake of clarity, the curves are shifted relatedly to zero

Despite the fact that the elemental analysis data, calculated for the hydrated compounds, agree well with the experimentally determined ones, by thermogravimetric analysis no water has been found in CoL_2 and ZnL_2 complexes. The compounds are stable to DTG onset of 236 and 207 °C (see Fig. 5), respectively, while the thermal stability of the anhydrous Cu(II) and Ni(II) complexes is significantly higher (329 and 271 °C, respectively). Above the onset temperatures, the decomposition of the anhydrous compounds is continuous and no intermediate formation is observed. The decomposition of all the compounds is practically finished up to 450 °C. The residue in nitrogen almost agrees with the amount for the pure metal (found: 17% Cu; 16% Co; 11% Ni–calcd. 12.11% Cu; 15.15%, Co; 13.08% Ni) except for the zinc complex 35% (calcd. 15.08% Zn).

The only endothermic process is the solvent evaporation in all the compounds, while the decomposition of the coordination compounds is highly exothermic in the whole decomposition range even in nitrogen flow. This is due to the high oxygen content of the ligand, and at elevated temperatures it is easily oxidized to water, carbon(IV) oxide and nitrogen oxide.

By coupled TG–MS measurements, the samples were checked for solvent. The TG–MS measurements, in accordance with the proposed composition, the results of elemental and thermogravimetric data, offer an additional proof for the presence of water in Cu(II) and Ni(II) complexes. Namely, the high intensity of the peaks for the ions with m/z = 18 and 17 and their intensity ratio agreeing with the NIST mass spectral data [28] unambiguously refer to the presence of water CuL_2 and NiL_2 compounds (Fig. 6a–d). On the contrary, in CoL_2 and ZnL_2 only traces of water can be found. This observation suggests the evaporation of the water during their storage. Due to high oxygen content of the ligand, in the following decomposition steps the same products were formed in all the cases: H_2O (m/z = 17 and 18), CO_2 (m/z = 44) and NO (m/z = 30).

Biological activity

The study on biological efficacy of the applied compounds in laboratory conditions was carried out on nutrient medium, potato dextrose agar (PDA), in Petri dishes of 90 mm in diameter. The water solutions of four complexes and a commercial fungicide (Table 4) were poured in the nutrient medium at a temperature of 60 °C. The test was repeated with five different concentrations of each compound in each repeated four times. The initial concentration of all compounds was 0.12%, and each subsequent composition was two times lower. Petri dishes poured with nutrient medium with no compounds added served as a control.

After the homogenization of the medium with the compound and agar solidification, mycelial fragments (6 mm in diameter) obtained from 10-day-old pure cultures

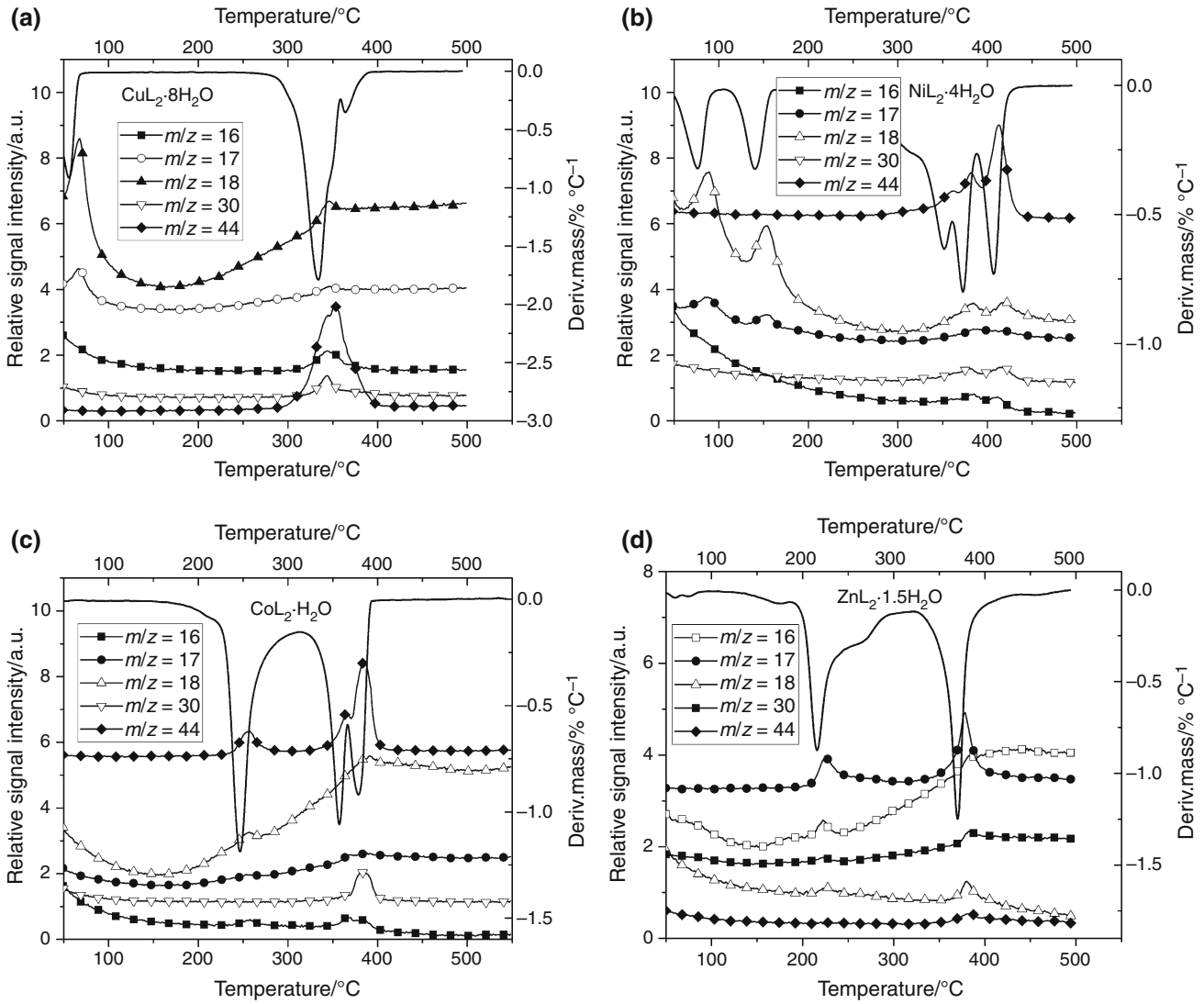

Fig. 6 Characteristic MS curves of the compounds $CuL_2{\cdot}8H_2O$ (**a**), $NiL_2{\cdot}4H_2O$ (**b**), CoL_2 (**c**), and ZnL_2 (**d**)

Table 4 Growth of *Ph. viticola* colonies (cm) and inhibitory effects of the studied compounds

Concentration/%	Studied compounds				
	Commercial fungicide	Cu complex	Ni complex	Co complex	Zn complex
0.12	0.0	6.0	3.4	3.8	5.4
0.06	0.0	6.4	6.4	4.3	6.7
0.03	0.0	6.4	6.5	5.4	6.8
0.015	0.0	6.4	6.6	5.6	6.8
0.0075	0.5	6.5	6.6	5.7	6.8
Control	6.9	6.9	6.9	6.9	6.9
$LSD_{0,01}$	0.112	0.149	0.298	0.266	0.222

of *Ph. viticola* were placed in the center of Petri dishes. Inoculated Petri dishes were maintained in an incubator at 25 °C. Mycelial growth of the fungus was measured when the colony in a control had covered about 2/3 of Petri dish diameter which was the case after 10 days.

A commercial fungicide expressed noticeably better inhibition effects than all complexes applied. All applied concentrations of commercial fungicide showed statistically significant inhibition to colony growth of *Ph. viticola*, in comparison with the control.

Studied complexes have not expressed such a distinguished inhibition as a commercial fungicide, although there were concentrations among them which have demonstrated a certain activity.

Conclusions

In the continuation of our systematic research of pyrazole coordination compounds, complexes of Cu(II), Ni(II), Co(II) and Zn(II) with 4-nitro-3-pyrazolecarboxylic acid ligand (L) were synthesized by four new complex compounds of formula $CuL_2{\cdot}8H_2O$, $NiL_2{\cdot}4H_2O$, $CoL_2{\cdot}H_2O$, $ZnL_2{\cdot}1.5H_2O$ with a pyrazole-based **L** = 4-nitro-3-pyrazolecarboxylic acid ligand (L). Bis(ligand) structures, ML_2 ($M = Cu^{II}$, Ni^{II}, Co^{II} and Zn^{II}), were proposed on the basis of elemental analysis, IR spectrometry, conductometric and TG–MS measurements. The low conductivity of the compounds additionally supports the deprotonation of the ligand and the formation of neutral complexes. The solvent content was calculated using the thermogravimetric (TG) data. In the case of solvates, elemental analysis data might be uncertain, as the amount of the solvent between the synthesis and the determination of the composition can be changed or even exchanged for water from the air. Therefore, TG–MS data in these cases are of crucial interest. In these complexes, TG/MS data gave unambiguous information about the presence of water and supported the obtained elemental analysis data. The crystal and molecular structures of $HL{\cdot}H_2O$ and $NH_4[LHL]$ were determined by single-crystal X-ray structure analysis; the asymmetric unit of $\mathbf{HL{\cdot}H_2O}$ consists of two independent 4-nitro-3-pyrazolecarboxylic acids molecules and two water molecules, all of them located in general positions. The asymmetric unit of **NH_4[LHL]** contains half of NH_4^+ cation and half of $[L{\cdots}H{\cdots}L]^-$ anion, as corresponding nitrogen and hydrogen atoms are situated at crystallographic inversion centers. A commercial fungicide expressed noticeably better inhibition effects than all complexes applied. All applied concentrations of commercial fungicide showed statistically significant inhibition to colony growth of *Ph. viticola*, in comparison with the control.

Acknowledgements A Hungary-Montenegro Intergovernmental Science and Technology Cooperation Programme Grant is acknowledged (TÉT_15-1-2016-0036). I. M. Szilágyi thanks for a János Bolyai Research Fellowship of the Hungarian Academy of Sciences and an ÚNKP-17-4-IV-BME-188 Grant supported by the ÚNKP-17-4-IV New National Excellence Program of the Ministry of Human Capacities, Hungary. A K 124212 Grant and an NRDI Grant 123631 are acknowledged. The research within Project No. VEKOP-2.3.2-16-2017-00013 was supported by the European Union and the State of Hungary, co-financed by the European Regional Development Fund.

References

1. Jaćimović ŽK, Giester G, Kosović M, Bogdanović GA, Novaković SB, Leovac VM, Latinović N, Barta Holló B, Mészáros Szécsényi K. Pyrazole-type complexes with Ni(II) and Cu(II). Solvent exchange reactions in coordination compounds. J Therm Anal Calorim. 2017;127(2):1501–9.
2. Ivanenkov YA, Balakin KV, Tkachenko SE. New approaches to the treatment of inflammatory disease: focus on small-molecule inhibitors of signal transduction pathways. Drugs R&D. 2008;9:397–434.
3. Graneto MJ, Kurumbail RG, Vazquez ML, Shieh HS, Pawlitz JL, Williams JM, Stallings WC, Geng L, Naraian AS, Koszyk FJ, Stealey MA, Xu XD, Weier RM, Hanson GJ, Mourey RJ, Compton RP, Mnich SJ, Anderson GD, Monahan JB, Devraj R. Synthesis, crystal structure, and activity of pyrazole-based inhibitors of p38 kinase. J Med Chem. 2007;50:5712–9.
4. Almeida da Silva PE, Ramosa DF, Bonacorso HG, Iglesia AI, Oliveira MR, Coelho T, Navarini J, Morbidoni HR, Zanatta N, Martins MAP. Synthesis and in vitro antimycobacterial activity of 3-substituted 5-hydroxy-5-trifluoro[chloro]methyl-4,5-dihydro-1H-1-(isonicotinoyl) pyrazoles. Int J Antimicrob Agents. 2008;32:139–44.
5. Reisner E, Arion VB, Keppler BK, Pombeiro AJL. Electron-transfer activated metal-based anticancer drugs. Inorg Chim Acta. 2008;361:1569–83.
6. Pruchnik FP, Jakimowicz P, Ciunik Z, Zakrzewska-Czerwińska J, Opolski A, Wietrzyk J, Wojdat E. Rhodium(III) complexes with polypyridyls and pyrazole and their antitumor activity. Inorg Chim Acta. 2002;334:59–66.
7. Sakai K, Tomita Y, Ue T, Goshima K, Ohminato M, Tsubomura T, Matsumoto K, Ohmura K, Kawakami K. Syntheses, antitumor activity, and molecular mechanics studies of cis-$PtCl_2(pzH)_2$ (pzH = pyrazole) and related complexes. Crystal structure of a novel Magnus-type double-salt $[Pt(pzH)_4][PtCl_4]$[cis-$PtCl_2(pzH)_2$]$_2$ involving two perpendicularly aligned 1D chains. Inorg Chim Acta. 2000;297:64–71.
8. Lemaire G, Mnif W, Pascussi JM, Pillon A, Rabenoelina F, Fenet H, Gomez E, Casellas C, Nicolas JC, Cavaillès V, Duchesne MJ, Balaguer P. Identification of new human pregnane X receptor ligands among pesticides using a stable reporter cell system. J Toxicol Sci. 2006;91:501–9.
9. Vicentini CB, Mares D, Tartari A, Manfrini M, Forlani G. Synthesis of pyrazole derivatives and their evaluation as photosynthetic electron transport inhibitors. J Agric Food Chem. 2004;52:1898–906.
10. Singh N, Sangwan NK, Dhindsa KS. Synthesis and fungitoxic activity of 5-aryl-1-formyl-4,5-dihydro-3-(2-hydroxyphenyl)-1*H*-pyrazoles and their complexes. Pest Manag Sci. 2000;56:284–8.
11. Barszcz B. Coordination properties of didentate N, O heterocyclic alcohols and aldehydes towards Cu(II), Co(II), Zn(II) and Cd(II) ions in the solid state and aqueous solution. Coord Chem Rev. 2005;249:2259–76.
12. Bol J. Synthetic models for dinuclear copper proteins, copper coordination compounds with macrocyclic pyrazolil ligands. Ph.D. Thesis, University Leiden, Leiden, Netherlands. 1997.
13. Schore NE. Study guide and solutions manual for organic chemistry: structure and function. 5th ed. San Francisco: Freeman WH and Company; 2007 **(in Serbian, 4th edition, Beograd, 2006, p. 429)**.
14. Bartyzel A. Synthesis, thermal behaviour and some properties of Cu(II) complexes with N, O-donor Schiff bases. J Therm Anal Calorim. 2017. https://doi.org/10.1007/s10973-017-6563-2.
15. de Oliveira EG, de Caland LB, de Oliveira AR, Machado PRL, Farias KJS, da Costa TR, Melo DMA, Cornélio AM, de Freitas

Fernandes-Pedrosa M, da Silva-Júnior AA. Monitoring thermal, structural properties, methotrexate release and biological activity from biocompatible spray-dried microparticles. J Therm Anal Calorim. 2017. https://doi.org/10.1007/s10973-017-6547-2.
16. Mohammad KA, Rahim SA, Bakar MRA. Kinetics and nucleation mechanism of carbamazepine–saccharin co-crystals in ethanol solution. J Therm Anal Calorim. 2017. https://doi.org/10.1007/s10973-017-6483-1.
17. Mahmoud WH, Mohamed GG, Mohamedin SYA. Spectroscopic characterization, thermal, antimicrobial and molecular docking studies on nano-size mixed ligand complexes based on sudan III azodye and 1,10-phenanthroline. J Therm Anal Calorim. 2017. https://doi.org/10.1007/s10973-017-6482-2.
18. Jaćimović ŽK, Giester G, Kosović M, Bogdanović GA, Novaković SB, Leovac VM, Latinović N, Barta Holló B, Mészáros Szécsényi K. Pyrazole-type complexes with Ni(II) and Cu(II). Solvent exchange reactions in coordination compounds. J Therm Anal Calorim. 2017;127:1501–9.
19. Stanković J, Lakić N, Ljubanović-Ralević I. Exercises in experimental statistics. University of Belgrade, Faculty of Agriculture. (1990), p. 242 (**in Serbian**).
20. Rigaku Oxford Diffraction. CrysAlisPro Software system, version 1.171.38.46; 2015.
21. Sheldrick GM. SHELXT—integrated space-group and crystal-structure determination. Acta Crystallogr Sect A Found Adv. 2015;71:3–8. https://doi.org/10.1107/S2053273314026370.
22. Sheldrick GM. Crystal structure refinement with *SHELXL*. Acta Crystallogr Sect C Struct Chem. 2015;71:3–8. https://doi.org/10.1107/S2053229614024218.
23. Hübschle CB, Sheldrick GM, Dittrich B. ShelXle: a Qt graphical user interface for SHELXL. J Appl Crystallogr. 2011;44:1281–4. https://doi.org/10.1107/S0021889811043202.
24. Spek AL. Structure validation in chemical crystallography. Acta Crystallogr Sect D Biol Crystallogr. 2009;65:148–55. https://doi.org/10.1107/S090744490804362X.
25. Macrae CF, Bruno IJ, Chisholm JA, Edgington PR, McCabe P, Pidcock E, et al. Mercury CSD 2.0—new features for the visualization and investigation of crystal structures. J Appl Crystallogr. 2008;41:466–70. https://doi.org/10.1107/S0021889807067908.
26. Farrugia LJ. WinGX and ORTEP for Windows: an update. J Appl Crystallogr. 2012;45:849–54. https://doi.org/10.1107/S0021889812029111.
27. Regiec A, Mastalarz H, Mastalarz A, Kochel A. Methylation of 4-nitro-3(5)-pyrazolecarboxylic acid. Tetrahedron Lett. 2009;50:2624–7. https://doi.org/10.1016/j.tetlet.2009.02.223.
28. http://webbook.nist.gov/. Accessed 07 July 2017.